Photodegradation of RDX in Aqueous Solution: A Mechanistic Probe for Biodegradation with Rhodococcus sp.

ARTICLE *in* ENVIRONMENTAL SCIENCE AND TECHNOLOGY · JANUARY 2003

Impact Factor: 5.33 · DOI: 10.1021/es0207753 · Source: PubMed

7 AUTHORS, INCLUDING:

Jalal Hawari
Université de Montréal-Ecole Polytechniqued
351 PUBLICATIONS **7,208** CITATIONS
SEE PROFILE

Annamaria Halasz
National Research Council Canada
83 PUBLICATIONS **2,634** CITATIONS
SEE PROFILE

Stéphane Deschamps
National Research Council Canada
10 PUBLICATIONS **324** CITATIONS
SEE PROFILE

Louise Paquet
National Research Council Canada
68 PUBLICATIONS **2,053** CITATIONS
SEE PROFILE

Environ. Sci. Technol. **2002**, *36,* 5117−5123

Photodegradation of RDX in Aqueous Solution: A Mechanistic Probe for Biodegradation with *Rhodococcus* sp.

J. HAWARI,* A. HALASZ, C. GROOM, S. DESCHAMPS, L. PAQUET, C. BEAULIEU, AND A. CORRIVEAU

Biotechnology Research Institute, National Research Council of Canada, 6100 Royalmount Avenue, Montreal, Quebec, H4P 2R2, Quebec, Canada

Recently we demonstrated that *Rhodococcus* sp. strain DN22 degraded hexahydro-1,3,5-trinitro-1,3,5-triazine (RDX) (**I**) aerobically via initial denitration followed by ring cleavage. Using UL ^{14}C-[RDX] and ring labeled ^{15}N-[RDX] approximately 30% of the energetic chemical mineralized (one C atom) and 64% converted to a dead end product that was tentatively identified as 4-nitro-2,4-diaza-butanal ($OHCHNCH_2NHNO_2$). To have further insight into the role of initial denitration on RDX decomposition, we photolyzed the energetic chemical at 350 nm and pH 5.5 and monitored the reaction using a combination of analytical techniques. GC/MS-PCI showed a product with a [M + H] at 176 Da matching a molecular formula of $C_3H_5N_5O_4$ that was tentatively identified as the initially denitrated RDX product pentahydro-3,5-dinitro-1,3,5-triazacyclohex-1-ene (**II**). LC/MS (ES-) showed that the removal of RDX was accompanied by the formation of two other key products, each showing the same [M − H] at 192 Da matching a molecular formula of $C_3H_7N_5O_5$. The two products were tentatively identified as the carbinol (**III**) of the enamine (**II**) and its ring cleavage product $O_2NNHCH_2NNO_2CH_2NHCHO$ (**IV**). Interestingly, the removal of **III** and **IV** was accompanied by the formation and accumulation of $OHCHNCH_2NHNO_2$ that we detected with strain DN22. At the end of the experiment, which lasted 16 h, we detected the following products HCHO, HCOOH, NH_2CHO, N_2O, NO_2^-, and NO_3^-. Most were also detected during RDX incubation with strain DN22. Finally, we were unable to detect any of RDX nitroso products during both photolysis and incubation with the aerobic bacteria, emphasizing that initial denitration in both cases was responsible for ring cleavage and subsequent decomposition in water.

Introduction

Hexahydro-1,3,5-trinitro-1,3,5-triazine (RDX) and octahydro-1,3,5,7-tetranitro-1,3,5,7-tetrazocine (HMX) are widely used explosives recognized to severely contaminate soil and groundwater (*1, 2*). Both RDX and HMX are toxic and mutagenic (*3*) and have the tendency to persist in contaminated environments (*4*). Recently Fournier et al. (*5*) employed *Rhodococcus* sp. strain DN22 isolated by Coleman et al. (*6*) in an effort to biodegrade the two explosives. We found that strain DN22 can degrade RDX effectively but is unable to degrade HMX. We achieved 30% mineralization, accounting for only one of the three C atoms in RDX, leaving the remaining two carbons in a dead end product that was identified as 4-nitro-2,4-diaza-butanal, O_2NNHCH_2NHCHO (*5*) (Figure 1). We suggested that initial enzymatic denitration of RDX during its incubation with strain DN22 was responsible for the destruction of the chemical in water. However, we were unable to detect the initial denitrated and other early intermediates considered important to the understanding of the degradation process (*5*).

Since initial enzymatic denitration of RDX was found sufficient to cause spontaneous decomposition, we hypothesized that photodenitration of the compound in water should also lead to spontaneous decomposition. Denitration of RDX by photolysis is presumed to be more rapid than enzymatic denitration and therefore might lead to the formation of sufficient amounts of intermediate products to allow detection.

Several studies reported the successful photodegradation of RDX, mostly via the homolysis of the N−NO_2 bond, under several oxidation conditions (*7*−*9*). In most reported cases, photodecomposition of RDX produces common secondary products including HCHO, HCOOH, NH_2CHO, NH_3, NO_2^-, NO_3^-, and N_2O. Interestingly most of these secondary photoproducts resembled those observed during aerobic degradation of RDX with strain DN22 (*5*) (Figure 1). The resemblance in product distribution between abiotic and biotic degradation of RDX indicates that once the molecule suffers a successful initial attack it undergoes rapid decomposition in water (*10*). However, these initial attacks and their resulting intermediate products are not well-known. We hope that the discovery of new RDX intermediates through a more rapid photodenitration technique can provide us with new insight into the initial enzymatic degradation mechanism(s) of cyclic nitramine explosives. Understanding the degradation pathways of RDX would help in the development of optimized (bio)remediation strategies for their removal.

Our objective is thus to photodenitrate RDX in deionized water at 350 nm in an attempt to generate sufficient amounts of initial intermediate(s) that we were unable to detect previously with *Rhodococcus* sp. strain DN22. We will conduct the photolysis experiments in nondegassed aqueous solutions at pH 5.5 and room temperature to mimic the conditions employed during RDX degradation with strain DN22 (*5*). The use of low energy wavelength light (350 nm) at neutral conditions was to minimize the formation of secondary photoproducts whose presence might interfere with other prime products considered important to the understanding of the degradation process. Some of the photolysis experiments were conducted in the presence of acetone in an attempt to enhance denitration through the energetic acetone triplet ($T_1(n,\pi^*)$) whose excitation energy equals to 326.04 KJ mol^{-1} (*11*).

Experimental Section

Chemicals. Commercial grade RDX (purity > 99%) was provided by the Defence Research Establishment Valcartier, Quebec, Canada (DREV). Acetone, formamide, and formaldehyde were from Aldrich, CA. Methylenedinitramine was from the rare chemical department of Aldrich, Canada. MNX with 98% purity was obtained from R. Spanggord (SRI, Menloe Park, CA), and TNX (99%) was obtained from G. Ampleman (DREV). All other chemicals used were of reagent grade.

* Corresponding author fax: (514)496-6265; e-mail: Jalal.Hawari@nrc.ca.

10.1021/es0207753 CCC: $22.00 Published 2002 by the Am. Chem. Soc.
Published on Web 11/02/2002

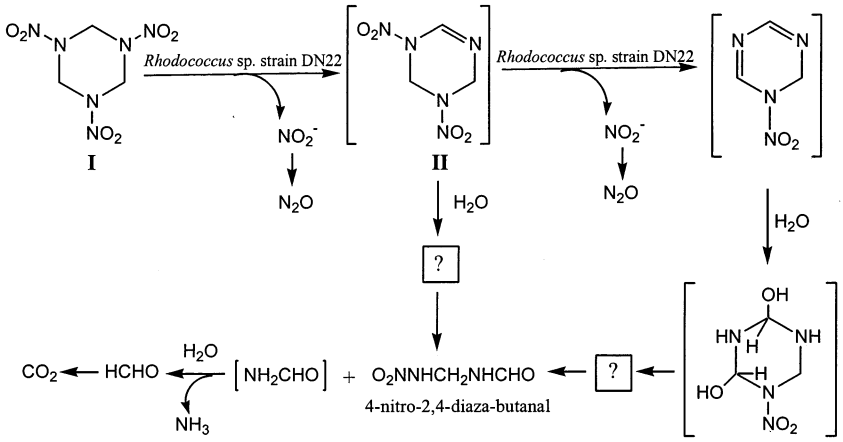

FIGURE 1. Proposed degradation routes of RDX by *Rhodococcus* sp. strain DN22 (*5*).

Irradiation Experiments. A Rayonet photoreactor RPR-100 fitted with a merry-go-round apparatus (Southern New England Co, Hamden, CT) equipped with sixteen 350 nm lamps were used as light sources. Photolysis was conducted in 20 mL tubes made of quartz. Each tube was charged with 10 mL of an aqueous solution of RDX (10 mg/L) in the presence and absence of acetone (250 ppm, v/v). Photolysis was carried out in nondegassed quartz tubes sealed with Teflon coated mininert valves. Controls containing RDX were kept in the dark during the course of the experiment. The temperature of the reactor was maintained at 25 °C by maintaining the apparatus in a cold room at 10 °C during irradiation. Light intensities, λ 350 = 3.0 10^{-6} einstein $ml^{-1}s^{-1}$ (RPR-350 nm lamp tubes emitting > 90% of their energy at 350 nm) were measured using ferrioxalate actinometry.

Degradation of RDX with *Rhodococcus* sp. Strain DN22. Experimental details on the biodegradation of RDX with strain DN22 can be found in Fournier et al. (*5*).

Analytical Procedures. Analysis of 3,5-dinitro-1,3,5-triazacyclohex-1-ene (**II**) was carried out on a Hewlett-Packard 6890 gas chromatograph coupled to a 5973 quadrupole mass spectrometer in the positive chemical ionization (PCI) mode using methane. Five μL of ethyl acetate extracts of the photolyzed mixture was injected in the solvent vent mode i.e., maintained at 10 °C 0.15 min then fast heated to 200 °C under splitless condition on a 15 m × 250 um × 0.5 um RTX-5 amine capillary column from Restek. Helium was used as the carrier gas under an average velocity of 27 cm/s. The column was heated at 55 °C for 3 min and then raised to 200 °C at a rate of 10 °C/min, and was held 2 min. The detector interface was maintained at 200 °C. The quadrupole and the source were held at 106 and 150 °C, respectively. The product was detected as its protonated molecular mass ion [M + H].

The cyclic carbinol intermediate (**III**), its ring cleavage product (**IV**), and their subsequent hydrolyzed products including methylenedinitramine (**VI**) (*12*) and 4-nitro-2,4-diaza-butanal (**V**) (*5*) were analyzed as described previously using LC/MS (ES-). Briefly, a Micromass benchtop single quadrupole mass detector attached to a Hewlett-Packard 1100 Series HPLC system and equipped with a photodiode array detector was used. The samples were injected into a Supelcosil LC-CN column (4.6 mm i.d. × 25 cm) (Supelco, Oakville, ON) at 35 °C. The solvent system consisted of acetonitrile (20%) in water at a flow rate of 1 mL/min. Ionization was done in a negative electrospray ionization mode ES (−) producing mainly the [M − H] mass ions. The mass range was scanned from 40 to 400 Da with a cycle time of 1.6 s, and the resolution was set to 1 Da (width at half-height) (*13*).

Formamide was derivatized with O-(2,3,4,5,6-pentafluorobenzyl)hydroxylamine.HCl (PFBHA) for 30 min at 80 °C and analyzed by LC/MS (ES-) using a 5 μm Supelcosil LC-8 column (4.6 mm ID × 25 cm) (Supelco, Oakville, ON) maintained at 35 °C. The solvent system consisted of acetonitrile/water gradient (50−90% v/v) at a flow rate of 1 mL/min. Detection was done by monitoring its [M − H] mass ions.

Formic acid, NO_2^-, and NO_3^- were measured using a HP^{3D} CE instrument model 1600 equipped with a diode array detector. The system was fitted with a Agilent G16006132 fused silica capillary with a total length of 64.5 cm (56 cm effective) and an internal diameter of 50 μm. The voltage was set at 25 kV (negative polarity) and the temperature at 25 °C. Samples were injected by applying 50 mbar pressure to the capillary inlet for 50 s. The electrolyte solution was prefiltered and buffered with triethanolamine at pH 7.7. Hexamethonium hydroxide is added as a cationic flow modifier. The separation time was 15 min. Indirect detection at 254 nm was used with pyromellitic acid as the background absorbing ion. The detection limit was 50 ppb.

Ammonium cation was analyzed using an SP 8100 HPLC system equipped with a Waters 431 conductivity detector and a Hamilton PRP-X200 (250 mm × 4.6 mm × 10 μm) analytical cation exchange column as described earlier (*14*). For trace analysis concentration of NH_4^+ was measured by capillary electrophoresis using a HP^{3D} CE instrument model 1600 equipped with a diode array detector. The system was fitted with an Agilent G16006132 fused silica capillary with a total length of 64.5 cm (56 cm effective) and an internal diameter of 50 um. The voltage was set at 15 kV (positive polarity) and the temperature at 25 °C. Samples were injected by applying 50 mbar pressure to the capillary inlet for 50 s. The electrolyte solution was prefiltered and buffered with lactic acid at pH 3.5 containing 18-crown-6 (50 mM). The separation time was 15 min. Indirect detection at 350 nm was used with imidazole as the background absorbing ion. Detection limit was 50 ppb.

Analysis of N_2O was carried out with a GC/ECD system as previously described (*13*).

Formaldehyde (HCHO) was analyzed as described by Summers (*15*) with a few modifications. Samples were derivatized with 2,4-pentanedione in the presence of ammonium acetate and glacial acetic acid for 1 h at pH 6.0, 40 °C. The derivatives were then analyzed by HPLC using a 5 μm Supelcosil LC-8 column (4.6 mm ID x 25 cm) (Supelco, Oakville, ON) maintained at 40 °C. The mobile phase consisted of an acetonitrile gradient of 15% to 27%, at a flow rate of 1.5 mL/min for 6 min. Detection and quantification were carried out using a fluorescence detector (excitation at 430 nm and emission at 520 nm).

Measurement of methanol is made on a Hewlett-Packard 6890 gas chromatograph coupled to an FID. 1 μL of aqueous

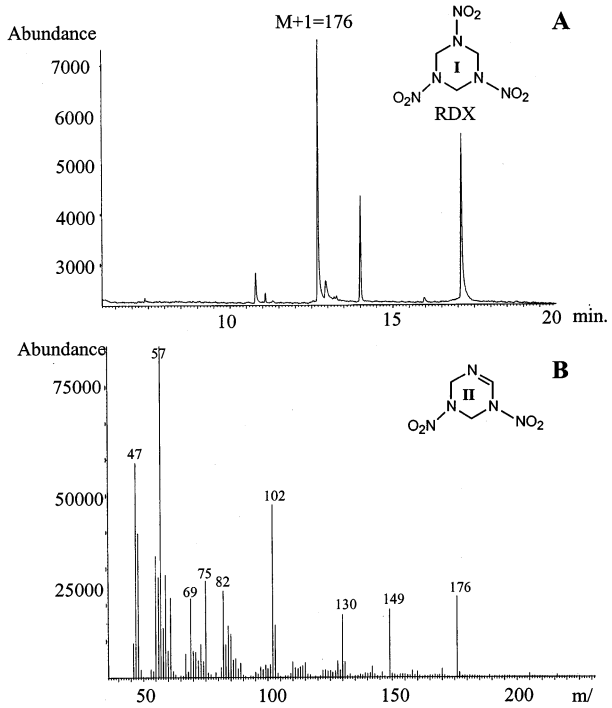

FIGURE 2. GC/MS (PCI) chromatogram of RDX after 2 h of photolysis at 350 nm (A) and mass spectrum of denitrated intermediate (II) at 12.7 min (B).

sample is injected on a 2 m × 0.03 mm Hayesep Q micropacked column from Supelco. The column is heated at 60 °C for 1 min and then raised to 180 °C at a rate of 20 °C/minute. Helium is used as carrier gas. The injector and detector are maintained at 150 °C and 250 °C, respectively. Standards are prepared from neat compounds from JT Baker. Detection limit is 0.25 ppm.

Results and Discussion

Photodegradation of RDX in Aqueous Solution at 350 nm. Figure 2A is a typical GC/MS (PCI) chromatogram of RDX after 2 h of photolysis at 350 nm showing a product with a retention time at 12.7 min and a protonated molecular mass ion [M + H] at 176 Da, matching a molecular formula of $C_3H_5N_5O_4$. The product also showed several other characteristic mass ions at 47, 102, and 149 Da representing $-HNO_2$, $CH_2NNO_2CH_2N$, and $O_2NHCH_2NNO_2CH_2N$, respectively (Figure 2B). The mass data of **II** matched exactly those of an earlier intermediate that was tentatively identified as pentahydro-3,5-dinitro-1,3,5-triaza-cyclohex-1-ene that we detected during hydrolysis of RDX in alkaline 2-propanol (*16*). Therefore we tentatively identified the present RDX photo product also as pentahydro-3,5-dinitro-1,3,5-triazacyclohex-1-ene. However, when we injected a standard material of RDX on the same GC we observed a peak that had the same retention time and [M + H] as that obtained during RDX photolysis. RDX is thermally unstable and decomposes via HNO_2 elimination (*17*), indicating that the energetic chemical might also undergo thermal decomposition at least partially during GC analysis. However, we found that the GC area of **II** generated during RDX photolysis was approximately twice as large as the area obtained from dark controls, suggesting its potential formation as a photo product. Several reports indicated the formation of **II** during photolysis, thermolysis, and hydrolysis of RDX (*8, 9, 16*−*18*), but as far as we are aware **II** has never been isolated. **II** is an enamine with a reactive −C═N bond that is expected to undergo rapid hydrolysis in water more likely to be unstable in water (*19*).

When we carried out photolysis in the presence of acetone, we detected two new LC/MS peaks marked **III** and **IV** at 18.2 and 6.8 min, respectively, as shown in Figure 3B. Each showed the same [M − H] at 192 Da, matching a molecular formula of $C_3H_7N_5O_5$ (MW 193 Da). The two products also showed several other characteristic mass ions at 46, 61, and 118 Da, representing $-NO_2$, $-NHNO_2$, and $-OHCNCH_2NHNO_2$ (Figure 4). Peak **III,** which appears next to RDX at a higher retention time, is presumed to be less polar and thus was tentatively identified as the cyclic carbinol hexahydro-2,4-dinitro-2,4,6-triazacyclohexanol (**III**) derivative of **II**, whereas peak **IV**, which appears at a lower retention time, was tentatively identified as the ring cleaved product 4,6-dinitro-2,4,6-triaza-hexanal ($O_2NNHCH_2NNO_2CH_2NHCHO$) of **III** (Figure 4). In the absence of acetone peaks **III** and **IV** were only detected in trace amounts.

We observed two other familiar intermediates, **V** at a retention time of 2.9 min with a [M − H] at 118 Da, matching a molecular formula of $C_2H_5N_3O_3$ and **VI** at a retention time of 2.3 min with a [M − H] at 135 Da matching a molecular formula of $CH_4N_4O_4$ (Figures 3 and 4). **V** was identified as 4-nitro-2,4-diaza-butanal by comparing its chromatographic and mass data with those of a standard material of $OHCNHCH_2NHNO_2$ obtained by incubating RDX with strain DN22 (*5*). Whereas **VI** was identified as methylenedinitramine, $O_2NNHCH_2NHNO_2$, by comparison with a commercial reference standard (Figures 3 and 4).

Interestingly, the LC/MS(ES-) spectrum of **IV** was found to contain a strong mass ion at 118 Da (Figure 4), suggesting that this intermediate might have acted as a precursor to O_2NNHCH_2NHCHO (**V**) whose [M − H] was also observed at 118 Da. Consequently, the dominant formation of **V** (64%) during biodegradation of RDX with *Rhodococcus* might thus suggest the direct involvement of intermediate **IV** in its formation too.

The last LC/MS (ES-) peak **VII** appearing at 3.9 min showed mainly a strong mass ion at 61 Da and was tentatively identified as the nitramide H_2NNO_2 (**VII**) (Figure 4). The spontaneous decomposition of **VII** in water produces nitrous oxide, N_2O (*10*).

The present mild photolysis (350 nm) of RDX in non-degassed aqueous solution did not produce any of the RDX nitroso derivatives such as MNX, DNX, and TNX. Interestingly none of the nitroso products was detected during RDX aerobic degradation with strain DN22 (*5, 6*). Fenton reagent (Fe^{2+}/H_2O_2), which is known to be a powerful generator of the highly reactive hydroxyl radicals, $OH^{\cdot}$, mineralized both RDX and HMX to CO_2 and NO_3^- without producing the nitroso compounds (*20*). However, photolysis of RDX at short wavelengths (higher energy) produced the nitroso derivatives (*9*). Nitroso products were frequently detected during biodegradation of RDX (*10, 21, 22*) under anaerobic conditions. Interestingly when we photolyzed RDX under a blanket of argon (anaerobic) at shorter wavelengths (254 nm) we detected all three nitroso products (unpublished data).

At the end of photolysis, which lasted 16 h, we observed the accumulation of the following products NO_2^-, NO_3^-, NH_2CHO, HCHO, HCOOH, N_2O, NO_2NHCH_2NHCHO, and $NO_2NHCH_2NHNO_2$. Most of these products were also detected during RDX incubation with the aerobic degrader DN22, emphasizing that once a successful initial attack takes place on RDX the molecule undergoes spontaneous decomposition in water (*10*).

The presence of acetone during RDX photolysis did not seem to drastically change product distribution. For instance, all products that were detected during RDX photolysis in the absence of acetone were also detected during its presence. Some slight variation in the relative distribution of these products was noted. Preliminary investigation with other photo sensitizers such as phenothiazine and benzyl viologen

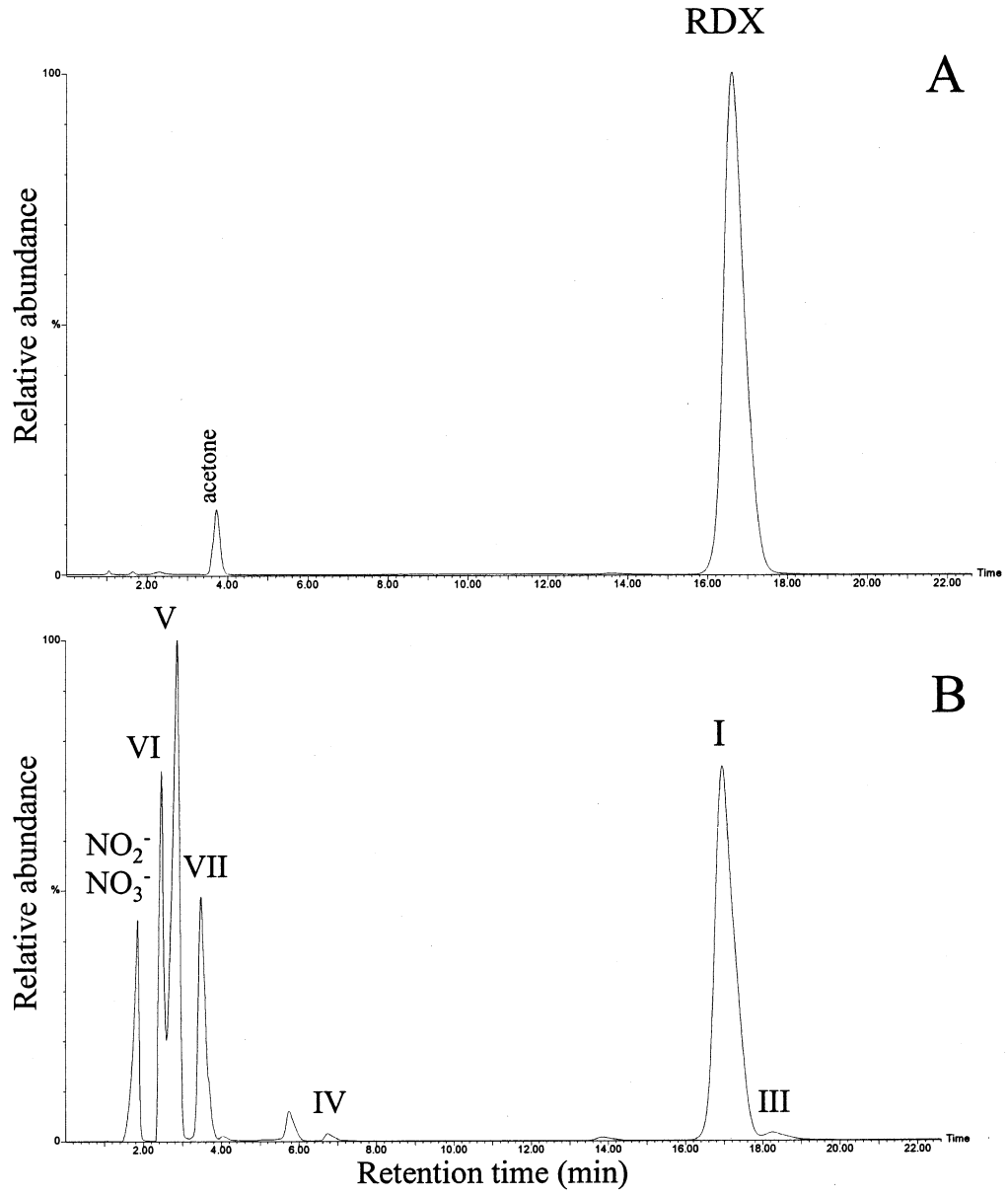

FIGURE 3. HPLC/UV chromatogram of RDX. A: before photolysis, B: after 3 h of photolysis at 350 nm.

also did not seem to drastically affect RDX product distribution. No RDX degradation was observed in dark aqueous controls with and without the sensitizer.

Kinetics and Stoichiometry: A Comparative Study with Strain DN22. The removal of RDX during photolysis was accompanied by the concurrent formation of nitrite NO_2^- and nitrate NO_3^- ions (Figure 5A). At the end of the experiment, which lasted 16 h, almost all of the NO_2^- transformed to NO_3^-, suggesting that nitrate ion was produced from nitrite photooxidation. For instance when we photolyzed $NaNO_2$ at 350 nm under the same conditions used to photolyze RDX we detected NO_3^-. Bose et al. (*8*) reported that photooxidation of RDX with ozone at 230 nm also produced nitrate. In contrast incubation of RDX with *Rhodococcus* strain DN22 produced NO_2^- without nitrate ion (*5*). The microorganism initiated enzymatic denitration to obtain nitrogen for growth since RDX was used as the sole source for nitrogen.

Photodegradation of RDX was also accompanied by the accumulation of NH_2CHO, HCHO, and HCOOH (Figure 5B). In the previous RDX biodegradation study with *Rhodococcus* we detected HCHO which later mineralized (liberated as $^{14}CO_2$), but NH_2CHO was inferred to exist by the detection of its degradation products ammonia and HCHO. For instance, when NH_2CHO was incubated with strain DN22 the amide degraded to ammonia and HCHO (*5*).

Figure 5A also showed that the removal of RDX was accompanied by the accumulation of the ring cleavage product 4-nitro-2,4-diaza-butanal (**V**), which was also detected during RDX biodegradation with DN22. However, **V** was found to persist indefinitely in incubation mixtures with strain DN22 at pH 7 but degraded slowly with light.

Table 1 shows that the N mass balance of RDX removal is 73% distributed as follows O_2NNHCH_2NHCHO (**V**) (22.2%), NO_2^- and NO_3^- (21.4%), NH_2CHO (15.7), N_2O (11.6%), and $CH_2(NHNO_2)_2$ (**VI**) (1.9%) and the C mass balance is 93% distributed as follows: NH_2CHO (31.5%), O_2NNHCH_2-NHCHO (**V**) (29.6%), HCHO (22.0%), HCOOH (9.1%), and $CH_2(NHNO_2)_2$ (**VI**) (0.9%). The nitrogen content of nitramide (NH_2NO_2) is not included in the N mass balance because of the absence of a standard material for quantification. In comparison, N- and C- mass balances of RDX biodegradation with strain DN22 were calculated as 90 and 94%, respectively (*5*). In the latter case approximately 30% of the C-content (1

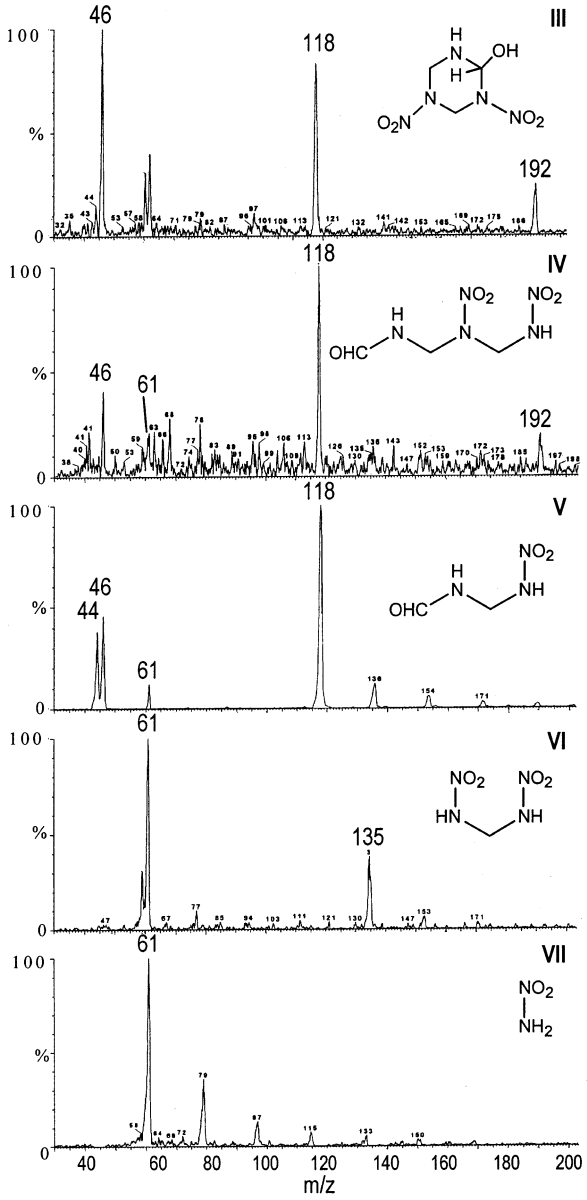

FIGURE 4. LC/MS (ES-) spectra of RDX degradation products III, IV, V, VI, and VII observed during photolysis at 350 nm in aqueous solution (see Figure 2B).

atom) of RDX was found in $^{14}CO_2$ and 64% (2 C atoms) was incorporated in the dead end product **V**. The slight differences in product distribution and N and C mass balances between photolysis and biodegradation experiments were possibly caused by some variations in the relative reactivities of certain intermediates toward light and enzymes.

Insights into the Photodecomposition Mechanism of RDX: The Parallel with Strain DN22. *Initial Denitration*. Figure 5A shows that the removal of RDX was concurrent with the formation of nitrite, NO_2^- (and NO_3^-), indicating the occurrence of an important initial denitration step during degradation. The absence of any of RDX nitroso products MNX, DNX, and TNX supported our belief that initial denitration was responsible for RDX subsequent degradation. Likewise, initial enzymatic denitration of RDX with *Rhodococcus* sp. strain DN22 was found sufficient to cause ring cleavage and subsequent decomposition in water (*5*).

During RDX photolysis in the presence of acetone, the ketone should produce a triplet $T_1(n,\pi^*)$ with excitation energy equals to 326.0 KJ mol^{-1} (*11*). Subsequent hydrogen atom

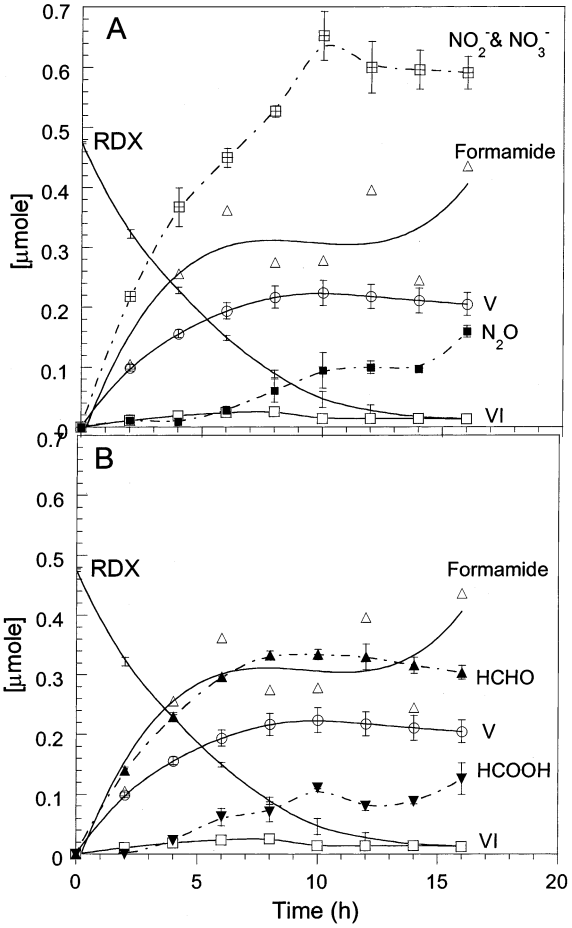

FIGURE 5. A time course of RDX photodegradation in aqueous solution at 350 nm. A: N-containing products. B: C-containing products. Error bars are based on triplicate measurements.

TABLE 1. Carbon and Nitrogen Mass Balances of RDX (0.46 µmol) after 16 h of Photolysis at 350 nm in Water

products	µmol ± SD	C-content %	N-content %
O_2NNHCH_2NHCHO (V)	0.205 ± 0.019	29.6	22.2
H_2NCHO	0.436[a]	31.5	15.7
$CH_2(NHNO_2)_2$ (VI)	0.013[a]	0.9	1.9
$NO_2^- + NO_3^-$	0.591 ± 0.027		21.4
N_2O	0.160 ± 0.009		11.6
HCHO	0.304 ± 0.011	22.0	
HCOOH	0.126 ± 0.026	9.1	
% mass balance		93.1	72.8

[a] Is a single measurement.

abstraction from one of RDX methylene groups by acetone $T_1(n,\pi^*)$ would generate an RDX radical RDX·. Elimination of NO_2 from RDX· should lead to the formation of the enamine **II**. This reaction is exothermic because the bond dissociation energies (BDE) of the cleaved C−H (in RDX) and the generated O−H (in acetone) bonds are 376.2 and 418.0 KJ mol^{-1}, respectively. However, the energy associated with acetone triplet $T_1(n,\pi^*)$ is high (326.0 KJ mol^{-1}) (*11*) and should be sufficient to cleave the N−NO_2 bond (BDE 204.9 KJ mol^{-1}). Alternatively, direct homolytic cleavage of the N−NO_2 bond in RDX should not be excluded. For instance the energy associated with λ 350 nm is 342 KJ mol^{-1} and therefore should be sufficient to cleave the N−NO_2 bond (BDE 204.9 KJ mol^{-1}) (*23*). However, a synchronous bimolecular elimination (E_2) of one molecule of HNO_2 during RDX photolysis has been suggested to occur (*9*, *24*). Nonetheless such elimination

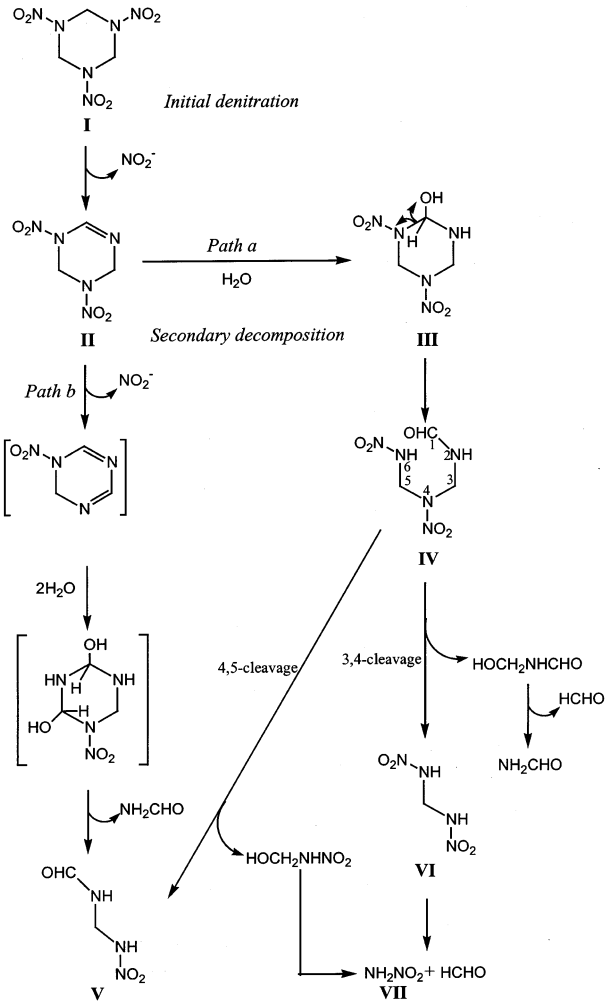

FIGURE 6. Postulated decomposition routes of RDX following its initial denitration by photolysis at 350 nm in an aqueous solution: a comparison with *Rhodococcus* sp. strain DN22 (Figure 1) (*5*). Path a cleavage following one denitration step and path b: cleavage following second denitration step.

would also lead to the formation of the enamine **II** (Figure 6). As we mentioned previously, the presence and absence of sensitizers such as acetone, phenothiazine, and benzyl viologen during RDX photolysis did not seem to change product distribution drastically. Therefore it is difficult to determine which among the previous denitration routes was the most probable one.

Secondary Decomposition. The potential involvement of the enamine **II** in the initial decomposition of RDX is supported by our observation of its carbinol derivative (**III**) and its subsequent ring cleavage product (**IV**) (Figure 6). As we mentioned previously enamines are unstable in water, and therefore **II** should react through its −C═N bond with an H_2O molecule to produce the carbinol **III.** The latter is also expected to be unstable and should undergo rapid ring cleavage across its NNO_2−CH(OH) to produce **IV** (Figure 6). For instance, α-hydroxylation of dialkylnitrosamine by mixed function oxidase produces unstable carbinol products that tend to cleave easily at the C(OH)-NNO_2 bond in water (*25*).

Intermediate **IV** with several labile C-NNO_2 bonds is thus expected to decompose in water to give several products depending on which bond is hydrolyzed first. For example 4,5-cleavage produces 4-nitro-2,4,-diaza-butanal (**V**), whereas 3,4 cleavage produces methylenedinitramine (**VI**) (Figure 6). Although we were unable to detect **III** and **IV** during RDX incubation with *Rhodococcus* (*5*), we now suggest their potential presence based on the predominant formation of their hydrolyzed product **V** (Figure 6). A high denitration rate should result in the formation of sufficient amounts of these early intermediates to permit detection. Subsequent reactions of these early intermediates in water is expected to be rapid and thus their product distribution will not be drastically influenced by light or enzyme.

After 16 h of photolysis we found that the disappearance of 0.46 μmol of RDX produced approximately 0.6 μmol of nitrite and nitrate ions, indicating that for every reacting molecule of RDX there was more than one N atom but less than two that were involved in the formation of nitrite (and nitrate) ion. Therefore we suggested the involvement of two denitration routes in the degradation of RDX: a mono denitration route leading to the formation of **II** (Figure 6, path a) and a second route which involved two denitration events prior to RDX ring cleavage (Figure 6, path b). In Figure 6, route a leads to the detected intermediates **IV**, **V**, **VI**, and **VII**, whereas route b leads to **V.** Previously we found that during RDX incubation with DN22 resting cells, there were two nitrite ions produced for each disappearing molecule of RDX, suggesting the involvement of the cyclic dicarbinol intermediate prior to ring cleavage (Figure 6, path b) (*5*). Our earlier hypothesis on the potential involvement of ring cleavage following the formation of the key intermediate **II** (Figure 1) (5) is now supported by the observation that products **III** and **IV** degrade further to form **V** without undergoing a second denitration (Figure 6, path a).

In conclusion Figure 6 represents the best explanation for the detected RDX degradation products obtained during photolysis and incubation of the chemical with *Rhodococcus* sp. DN22. Figure 6 clearly shows that the reaction steps involved in the photodecomposition of RDX are replicates of those occurring during biodegradation of the energetic chemical under aerobic conditions with strain DN22. These findings are in accordance with our earlier hypothesis, which emphasizes that once a successful initial enzymatic or chemical attack, denitration in the present study, occurs on RDX (or HMX), the energetic chemical will decompose rapidly in water (*10*). Our hypothesis is proven through the obtention of similar product distribution (NO_2^-, N_2O, NH_2CHO, HCHO, HCOOH, and O_2NNHCH_2NHCHO) in both cases. However, the enzyme that initiated the attack on RDX to perform denitration is still unknown and certainly requires further investigation (*5, 6*).

Acknowledgments

We are grateful to Sonia Thiboutot and Guy Ampleman from the Defense Research Establishment Valcartier, Quebec, Canada for providing us with the energetic chemicals. We also thank Dr. Jim Spain for his valuable discussion. Finally we would like to thank Philomena D'Cruz for her technical assistance. Funding was provided by the U.S. DoD/DoE/EPA Strategic Environmental Research and Development Program (SERDP CU1213). This is NRCC Publication 45887.

Literature Cited

(1) Myler C. A.; Sisk, W. In *Environmental Biotechnology for Waste Treatment;* Sayler, G. S., Fox, R., Blackburn, J. W., Eds.; Plenum Press: NY, 1991; pp 137−146.

(2) Haas, R.; Schreiber, I.; v. Löw, E.; Stork G. *Fresenius J. Anal. Chem.* **1990,** *338,* 41.

(3) Robidoux, P. Y.; Svedsen, C.; Caumartin, J.; Hawari, J.; Ampleman, G.; Thiboutot, S.; Weeks, J. M.; Sunahara, I. *Environ. Toxic. Chem.* **2000**, *19*, 1764.

(4) Kaplan, D. L. *Curr. Opin. Biotechnol.* **1992**, *3*, 253.

(5) Fournier, D.; Halasz, A.; Spain, J.; Fiurasek, P.; Hawari, J. *Appl. Environ. Microbiol.* **2002**, *68*, 166.

(6) Coleman, N. V.; Nelson, D. R.; Duxbury, T. *Soil Biol. Biochem.* **1998,** *30*, 1159.

(7) Kubose, D. A.; Hoffsommer, J. C. *Technical Report 77-20*, ADA 042199, Naval Surface Weapons Center, White Oak Laboratory, Silver Spring, MD, 1977.
(8) Bose, P.; Glaze, W. H.; Maddox, S. *Water Res.* **1998**, *32*, 1005.
(9) Peyton, G. R.; LeFaivre, M. H.; Maloney, S. W. *CERL Technical Report 99/93*, (www.CECER.Army/TechReports)0.1999.
(10) Hawari, J. In *Biodegradation of nitroaromatic compounds and explosives*; Spain, J. C., Hughes, J. B., Knackmuss, H.-J., Eds.; CRC Press: Boca Raton, FL, 2000; pp 277−310.
(11) Turro, N. J. *Modern Molecular Photochemistry*; Benjamin Cumming Publishing Co.: 1978; Chapter 10, p 362.
(12) Halasz, A.; Spain, J.; Paquet, L.; Beaulieu, C.; Hawari J. *Environ. Sci. Technol.* **2002**, *36*, 633.
(13) Hawari, J.; Halasz, A.; Sheremata, T.; Beaudet, S.; Groom, C.; Paquet, L.; Rhofir, C.; Ampleman, G.; Thiboutot, S. *Appl. Environ. Microbiol.* **2000**, *66*, 2652.
(14) Hawari, J.; Halasz, A.; Beaudet, S.; Paquet, L.; Ampleman, G.; Thiboutot, S. *Environ. Sci. Technol.* **2001**, *35*, 70.
(15) Summers, W. R. *Anal. Chem.* **1990**, *62*, 1397.
(16) Hawari, J.; Paquet, L.; Zhou, E.; Halasz, A.; Zilber B. *Chemosphere* **1996**, *32*, 1929.
(17) Zhao, X.; Hintsa, E. J.; Lee, Y. T. *J. Chem. Phys.* **1988**, *88*, 801.
(18) Hoffsommer, J. C.; Kubose, D. A.; Glover, D. J. *J. Phys. Chem.* **1977**, *81*, 380.
(19) March, J. *Advanced organic chemistry*, 3rd ed.; Wiley-Interscience Publication, John Wiley & Sons: New York, U.S.A., 1985; pp 784−785.
(20) Zoh, K.; Stenstrom, M. K. *Water Res.* **2002**, *36*, 1331.
(21) McCormick, N. G.; Cornell, J. H.; M. Kaplan; A. *Appl. Environ. Microbiol.* **1981**, *42*, 817.
(22) Oh, B. T.; Just, C. L.; Alvarez, P. J. *Environ. Sci. Technol.* **2001**, *35*, 4341.
(23) Behrens, R. Jr.; Bulusu, S. *J. Phys. Chem.* **1991**, *95*, 5838.
(24) Melius, C. F. In *Chemistry and Physics of Energetic Materials;* Bulusu S. N., Ed.; Kluwer Academic Publishers: Netherlands, 1990; pp 21−49.
(25) Druckrey, H. *Xenobiotica* **1973**, *3*, 271.

Received for review June 7, 2002. Revised manuscript received September 9, 2002. Accepted September 10, 2002.

ES0207753